How an internal supramolecular interaction determines the stereochemistry of a metal center

Maxime Steinmetz, Christophe Gourlaouen and David Séméril

Contents

Materials and Methods

All synthetic reactions were carried out under argon. Routine ^{1}H, $^{13}C\{^{1}H\}$, $^{31}P\{^{1}H\}$ and $^{19}F\{^{1}H\}$ spectra were recorded with Bruker FT instruments (AC 300 and 500). ^{1}H, ^{13}C NMR spectroscopic data were referenced to residual protonated solvents (δ = 2.50 ppm and 39.52 ppm for DMSO-d_6, respectively, and 7.26 ppm and 77.16 ppm for $CDCl_3$, respectively). ^{31}P and ^{19}F NMR spectroscopic data were given relative to external H_3PO_4 and CCl_3F, respectively. Chemical shifts and coupling constants are reported in ppm and Hz, respectively. Infrared spectra were recorded with a Bruker FT-IR Alpha-P spectrometer. Mass spectra were recorded on a Bruker MicroTOF spectrometer (ESI-TOF). Elemental analyses were carried out by the Service de Microanalyse, Institut de Chimie, Université de Strasbourg. 5-Phenyl-1,3,4-oxadiazol-2-amine was prepared by literature procedure [Niu, P.; Kang, J.; Tian, X.; Song, L.; Liu, H.;Wu, J.; Yu,W.; Chang, J. Synthesis of 2-amino-1,3,4-oxadiazoles and 2-amino-1,3,4-thiadiazoles via sequential condensation and I2-mediated oxidative C-O/C-S bond formation. *J. Org. Chem*. **2015**, *80*, 1018-1024].

(*E*)-1-Phenyl-*N*-(5-phenyl-1,3,4-oxadiazol-2-yl)methanimine (1)

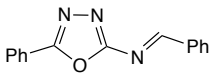

In a round bottomed flask equipped with a Dean Stark apparatus, a mixture of phenyl-1,3,4-oxadiazol-2-amine (10.0 mmol) and benzaldehyde (15.0 mmol) in toluene (100 mL) was refluxed for 20 h. After cooling to room temperature, the solvent was evaporated and the crude product was washed with cool ethanol (30 mL), filtered and dried under vacuum to afford the desired imine as a white solid in yield 24 %. ^{1}H NMR (300 MHz, DMSO-d$_6$): δ = 9.37 (s, 1H, N=CH), 8.14-8.06 (m, 4H, arom. CH), 7.74-7.60 (m, 6H, arom. CH) ppm; ^{13}C{^{1}H} NMR (126 MHz, DMSO-d$_6$): δ = 170.22 (s, N=CH), 166.19 (s, arom. Cquat C(N)=N), 162.84 (s, arom. Cquat C(Ph)=N), 134.32 (s, arom. Cquat), 134.26 (s, arom. CH), 132.03 (s, arom. CH), 130.33 (s, arom. CH), 129.47 (s, arom. CH), 129.34 (s, arom. CH), 126.42 (s, arom. CH), 123.54 (s, arom. Cquat) ppm. Elemental analysis calcd. (%) for $C_{15}H_{11}ON_3$ (249.27): C 72.28, H 4.45, N 16.86; found C 72.32, H 4.47, N 16.82.

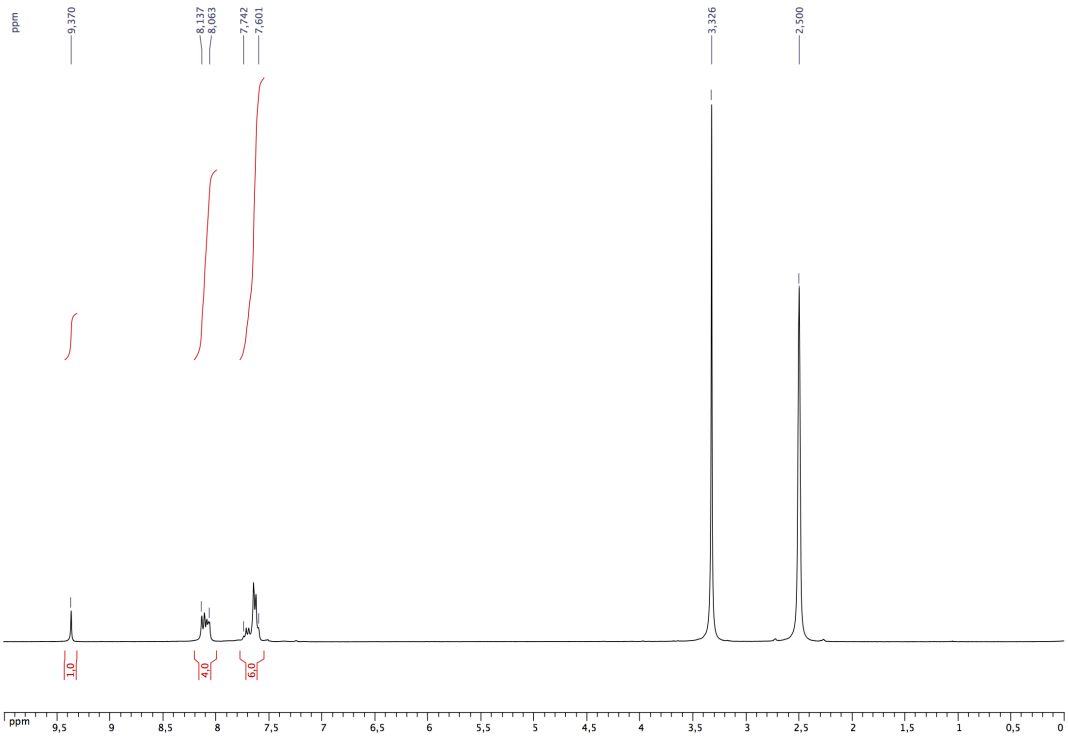

Figure S1. ^{1}H NMR spectrum (DMSO-d$_6$)

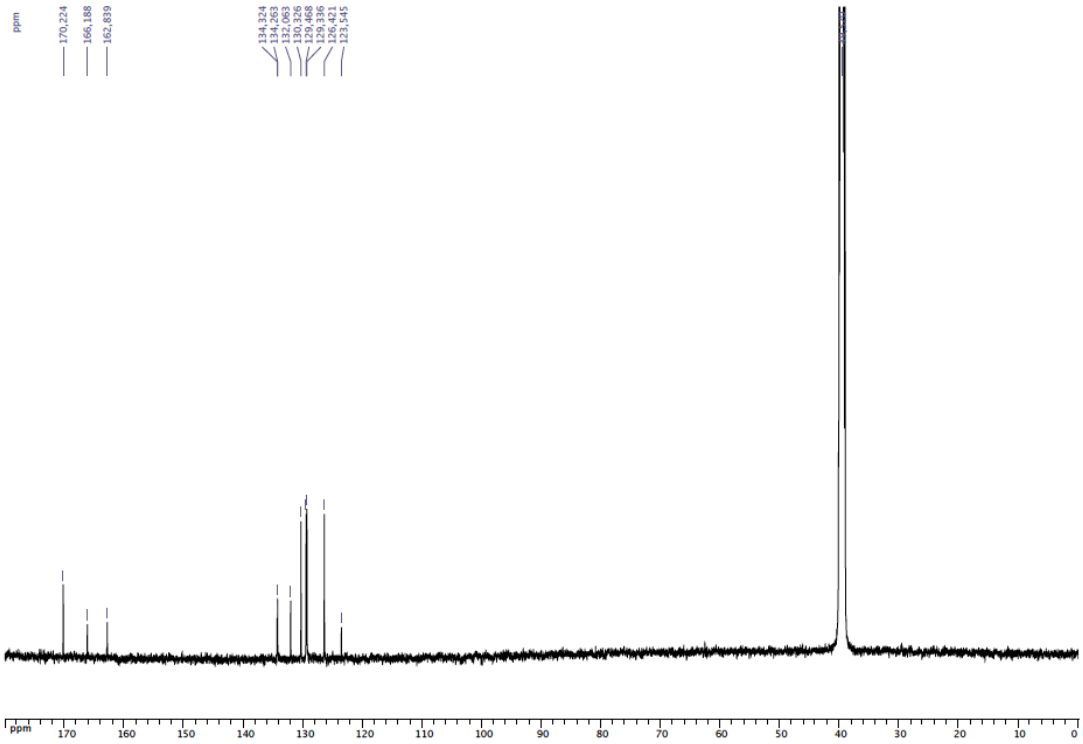

Figure S2. $^{13}C\{^{1}H\}$ NMR spectrum (DMSO-d_6)

Diphenylphosphanyl-[(5-phenyl-1,3,4-oxadiazol-2-ylamino)phenyl-methyl] borane (2)

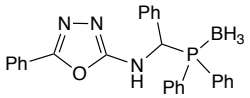

In a Schlenk tube, *n*-butyllithium (1.6 M in hexane, 1.20 mL, 1.92 mmol) was rapidly added to a solution of borane-diphenylphosphine complex (400 mg, 2.00 mmol) in THF (50 mL) at -78°C. After 5 minutes, the solution was heated to 0°C and the reaction mixture was stirred for an additional time of 0.5 h. The generated anion was then cannulated to a solution of imine **1** (496 mg, 1.90 mmol) in THF (50 mL) and the reaction was stirred at room temperature for 16 h. The solution was quenched with water (100 mL) and the aqueous layer was extracted with CH_2Cl_2 (3 x 50 mL). The combined organic layers were washed with water (2 x 50 mL), brine (50 mL), dried over $MgSO_4$ and filtered. The solvent was then evaporated under reduced pressure and the crude product was purified by column chromatography (CH_2Cl_2; *R*f = 0.22) to give the compound **2** as white solid in 61 % yield (520 mg). ^{1}H NMR (500 MHz, $CDCl_3$): δ = 8.08-8.04 (m, 2H, arom. CH), 7.93 (dd, 2H, arom. CH, $^3J_{HH}$ = 7.0 Hz, $^4J_{HH}$ = 2.0 Hz), 7.67-7.60 (m, 3H, arom. CH), 7.53-7.48 (m, 4H, arom. CH), 7.47-7.42 (m, 3H, arom. CH), 7.36 (td, 2H, arom. CH, $^3J_{HH}$ = 7.8 Hz, $^4J_{HH}$ = 2.5 Hz), 7.30-7.25 (m, 4H, arom. CH), 6.16 (dd, 1H, NH, $^3J_{HH}$ = 10.0 Hz, $^3J_{PH}$ = 4.5 Hz), 6.07 (dd, 1H, CHP, $^2J_{PH}$ = 15.0 Hz, $^3J_{HH}$ = 10.0 Hz), 1.49-0.92 (br s, 3H, BH_3) ppm; ^{13}C{^{1}H} NMR (126 MHz, $CDCl_3$): δ = 161.88 (d, arom. Cquat CH(*C*)PPh_2, $^2J_{CP}$ = 11.0 Hz), 159.90 (s, arom. Cquat C(Ph)=N), 134.17 (d, arom. Cquat C(NH)=N, $^3J_{CP}$ = 4.8 Hz), 133.33 (d, arom. CH of P(C_6H_5)$_2$, $^2J_{CP}$ = 8.9 Hz), 132.75 (d, arom. CH of P(C_6H_5)$_2$, $^2J_{CP}$ = 8.9 Hz), 132.16 (d, arom. CH of P(C_6H_5)$_2$, $^4J_{CP}$ = 2.5 Hz), 131.99 (d, arom. CH of P(C_6H_5)$_2$, $^4J_{CP}$ = 2.5 Hz), 130.92 (s, arom. CH of C(C_6H_5)=N), 129.38 (d, arom. CH of P(C_6H_5)$_2$, $^3J_{CP}$ = 10.0 Hz), 128.98 (s, arom. CH of C(C_6H_5)=N), 128.66 (d, arom. CH of P(C_6H_5)$_2$, $^3J_{CP}$ = 10.5 Hz), 128.58 (d, arom. CH of CH(*C*$_6H_5$)PPh_2, $^5J_{CP}$ = 2.4 Hz), 128.52 (d, arom. CH of CH(*C*$_6H_5$)PPh_2, $^4J_{CP}$ = 3.8 Hz), 128.18 (d, arom. CH of CH(*C*$_6H_5$)PPh_2, $^3J_{CP}$ = 1.9 Hz), 127.43 (d, arom. Cquat of P(C_6H_5)$_2$, $^1J_{CP}$ = 81.4 Hz), 126.16 (d, arom. Cquat of P(C_6H_5)$_2$, $^1J_{CP}$ = 77.0 Hz), 126.04 (s, arom. CH of C(C_6H_5)=N), 124.20 (s, arom. Cquat of C(C_6H_5)=N), 54.06 (d, CHP, $^1J_{CP}$ = 41.0 Hz) ppm; ^{31}P{^{1}H} NMR (121 MHz, $CDCl_3$): δ = 26.5 (br s, P(BH_3)Ph_2) ppm; IR: ν = 1605 cm^{-1} (C=N). Elemental analysis calcd. (%) for $C_{27}H_{25}ON_3PB$ (449.30): C 72.18, H 5.61, N 9.35; found C 71.97, H 5.56, N 9.27.

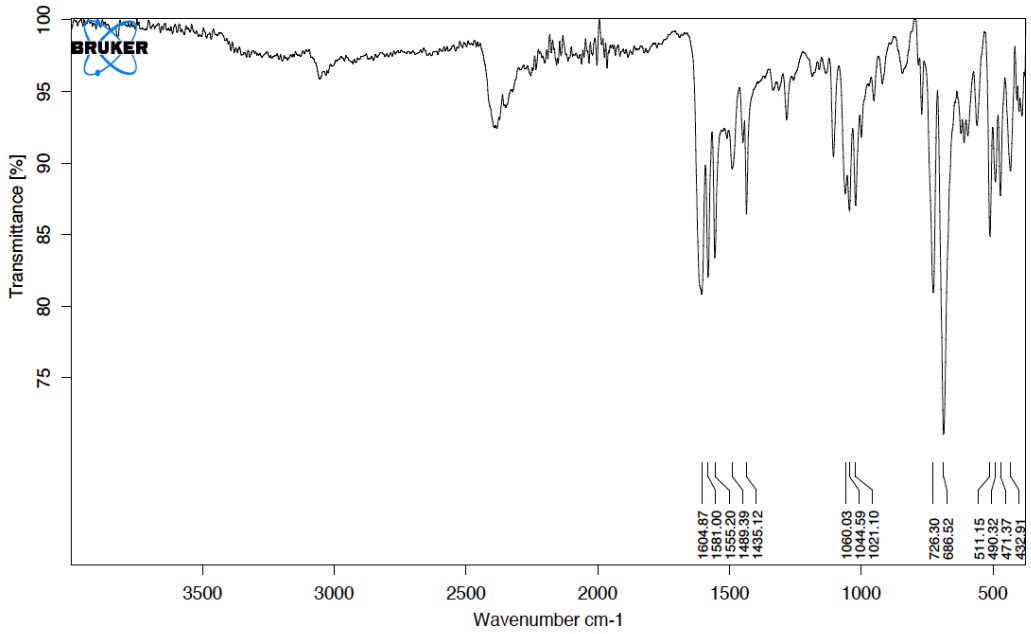

Figure S3. FT-IR spectrum

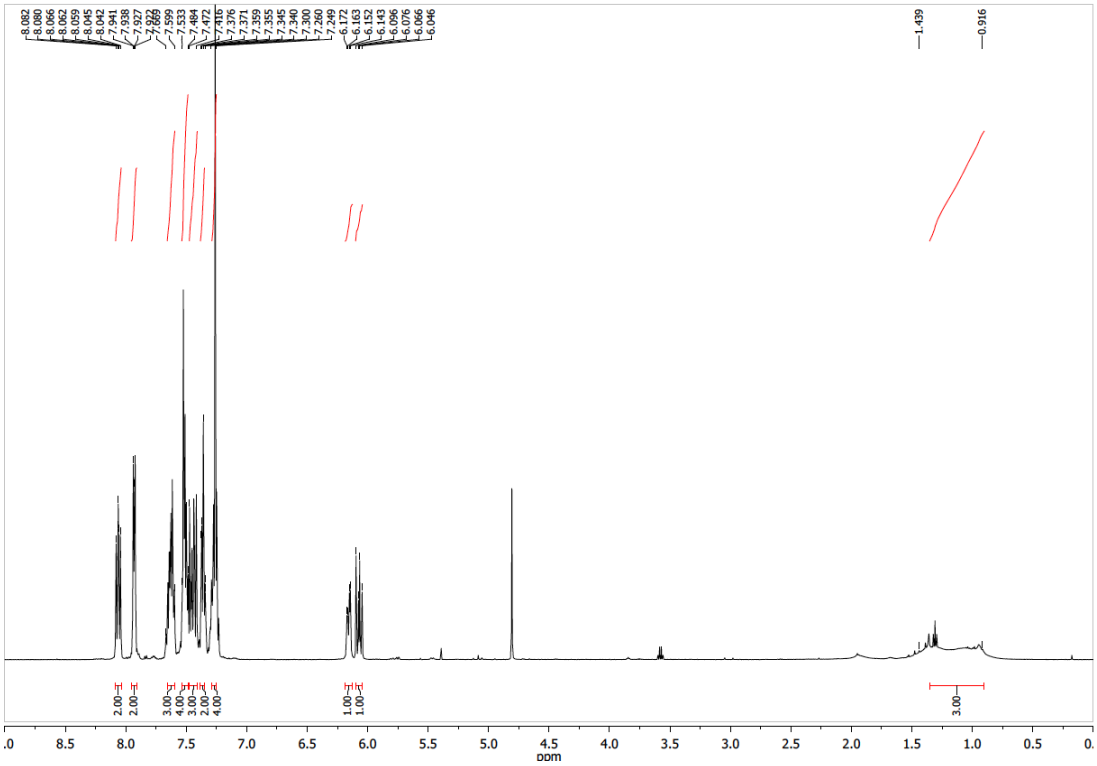

Figure S4. ^{1}H NMR spectrum ($CDCl_3$)

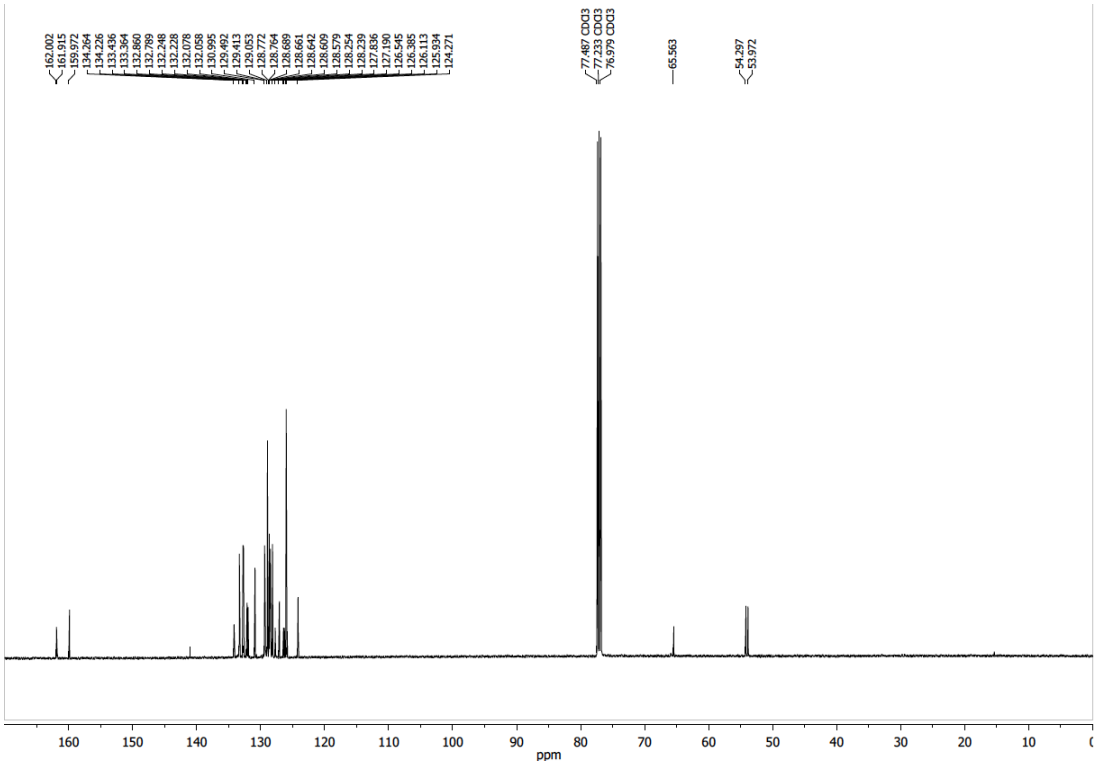

Figure S5. $^{13}C\{^{1}H\}$ NMR spectrum ($CDCl_3$)

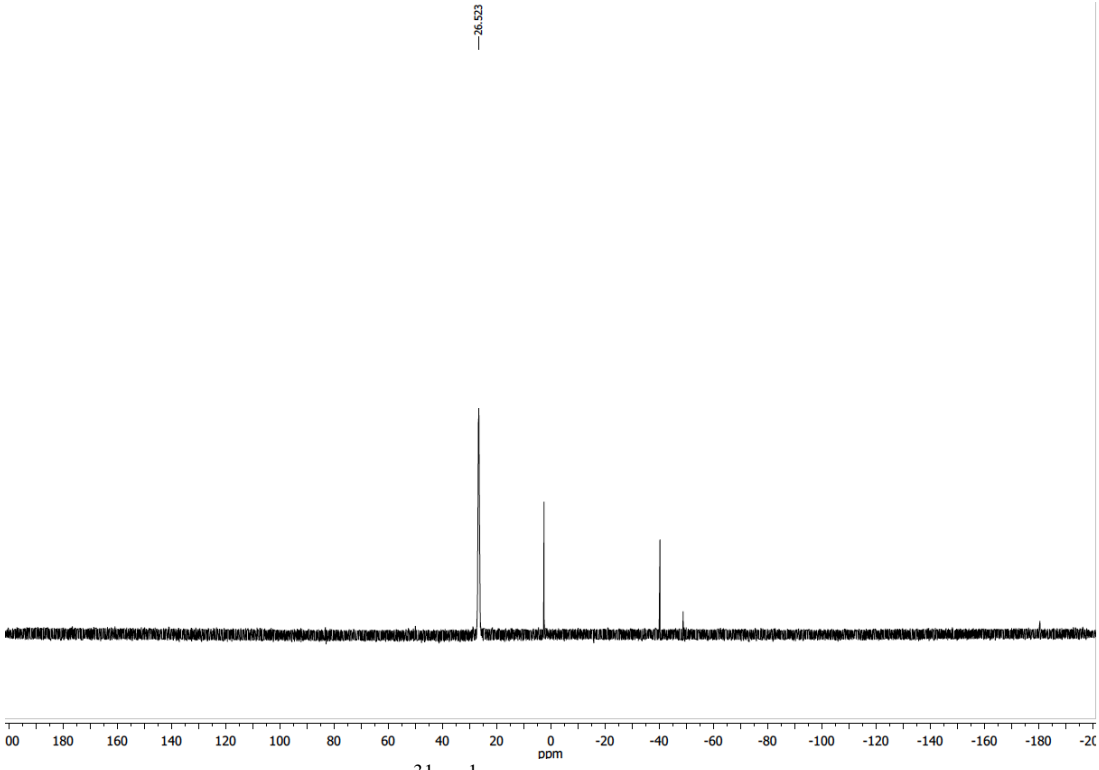

Figure S6. $^{31}P\{^{1}H\}$ NMR spectrum ($CDCl_3$)

Dichloro-*N*-{diphenylphosphanyl-[(5-phenyl-1,3,4-oxadiazol- 2-ylamino)phenyl-methyl] borane}(p-cymene)ruthenium(II) (3)

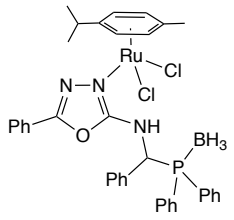

A solution of phosphanyl borane (**2**) (0.099 g, 0.22 mmol) in CH_2Cl_2 (50 mL) was added dropwise to a stirred solution of $[RuCl_2(p\text{-cymene})]_2$ (0.067 g, 0.11 mmol) in CH_2Cl_2 (200 mL). The reaction mixture was further stirring at room temperature for 4 h. The solution was then concentrated to *ca*. 1 mL, upon which *n*-hexane (50 mL) was added. The orange/red precipitate was separated by filtration, washed with hexane (10 mL) and dried under vacuum to afford the complex **3** as an orange/red solid in 92 % yield (152 mg). ^{1}H NMR (500 MHz, $CDCl_3$): δ = 8.47 (dd, 1H, NH, $^3J_{HH}$ = 9.0 Hz, $^3J_{PH}$ = 2.0 Hz), 7.97-7.93 (m, 2H, arom. CH), 7.88-7.84 (m, 2H, arom. CH), 7.66-7.64 (m, 2H, arom. CH), 7.52-7.41 (m, 6H, arom. CH), 7.36-7.34 (m, 3H, arom. CH), 7.21-7.16 (m, 5H, arom. CH), 5.61 and 5.31 (AA'BB' spin system, 2H, arom. CH of *p*-cymene, $^3J_{HH}$ = 6.5 Hz, $^4J_{HH}$ = 1.5 Hz), 5.58 and 5.31 (AA'BB' spin system, 2H, arom. CH of *p*-cymene, $^3J_{HH}$ = 6.0 Hz, $^4J_{HH}$ = 1.5 Hz), 5.48 (dd, 1H, arom. CHP, $^2J_{PH}$ = 9.2 Hz, $^3J_{HH}$ = 6.5 Hz), 3.09 (hept, 1H, C*H*$(CH_3)_2$, $^3J_{HH}$ = 7.0 Hz), 2.26 (s, 3H, CH_3 of *p*-cymene), 1.29 (d, 3H, CH(C*H*$_3)_2$, $^3J_{HH}$ = 7.0 Hz), 1.27 (d, 3H, CH(C*H*$_3)_2$, $^3J_{HH}$ = 7.0 Hz), 1.20-0.58 (br s, 3H, BH_3) ppm; ^{13}C{^{1}H} NMR (126 MHz, $CDCl_3$): δ = 162.03 (d, arom. Cquat CH(*C*)PPh_2, $^2J_{CP}$ = 4.3 Hz), 156.51 (s, arom. Cquat C(Ph)=N), 135.03 (d, arom. CH of $P(C_6H_5)_2$, $^2J_{CP}$ = 9.2 Hz), 134.00 (d, arom. CH of $P(C_6H_5)_2$, $^2J_{CP}$ = 8.9 Hz), 133.54 (d, arom. Cquat C(NH)=N, $^3J_{CP}$ = 1.6 Hz), 132.25 (d, arom. CH of $P(C_6H_5)_2$, $^4J_{CP}$ = 2.5 Hz), 131.70 (d, arom. CH of $P(C_6H_5)_2$, $^4J_{CP}$ = 2.5 Hz), 131.60 (s, arom. CH of $C(C_6H_5)$=N), 129.13 (s, arom. CH of $C(C_6H_5)$=N), 128.96 (d, arom. CH of $P(C_6H_5)_2$, $^3J_{CP}$ = 10.2 Hz), 128.80 (d, arom. CH of $P(C_6H_5)_2$, $^3J_{CP}$ = 10.0 Hz), 128.63 (d, arom. CH of CH(*C*$_6$H$_5$)PPh_2, $^4J_{CP}$ = 4.0 Hz), 128.45 (d, arom. CH of CH(*C*$_6$H$_5$)PPh_2, $^5J_{CP}$ = 2.6 Hz), 128.05 (d, arom. CH of CH(*C*$_6$H$_5$)PPh_2, $^3J_{CP}$ = 2.1 Hz), 126.25 (d, arom. Cquat of $P(C_6H_5)_2$, $^1J_{CP}$ = 53.5 Hz), 125.94 (s, arom. CH of $C(C_6H_5)$=N), 123.23 (d, arom. Cquat of $P(C_6H_5)_2$, $^1J_{CP}$ = 52.5 Hz), 122.87 (s, arom. Cquat of $C(C_6H_5)$=N), 102.92 (s, arom. Cquat of *p*-cymene), 98.95 (s, arom. Cquat of *p*-cymene), 84.03 (s, arom. CH of *p*-cymene), 81.35 (s, arom. CH of *p*-cymene), 81.18 (s, arom. CH of *p*-cymene), 59.43 (d, CHP $^1J_{CP}$ = 30.1 Hz), 30.78 (s, *C*H$(CH_3)_2$), 22.46 (s, CH(*C*$H_3)_2$), 22.32 (s, CH(*C*$H_3)_2$), 18.90 (s, CH_3 of *p*-cymene) ppm; ^{31}P{^{1}H} NMR (121 MHz, $CDCl_3$): δ = 26.1 (br s, $P(BH_3)Ph_2$) ppm; IR: ν = 1632 cm^{-1} (C=N). Elemental analysis calcd. (%) for $C_{37}H_{39}ON_3PBRuCl_2$ (249.27): C 58.82, H 5.20, N 5.56; found C 58.94, H 5.62, N 5.41.

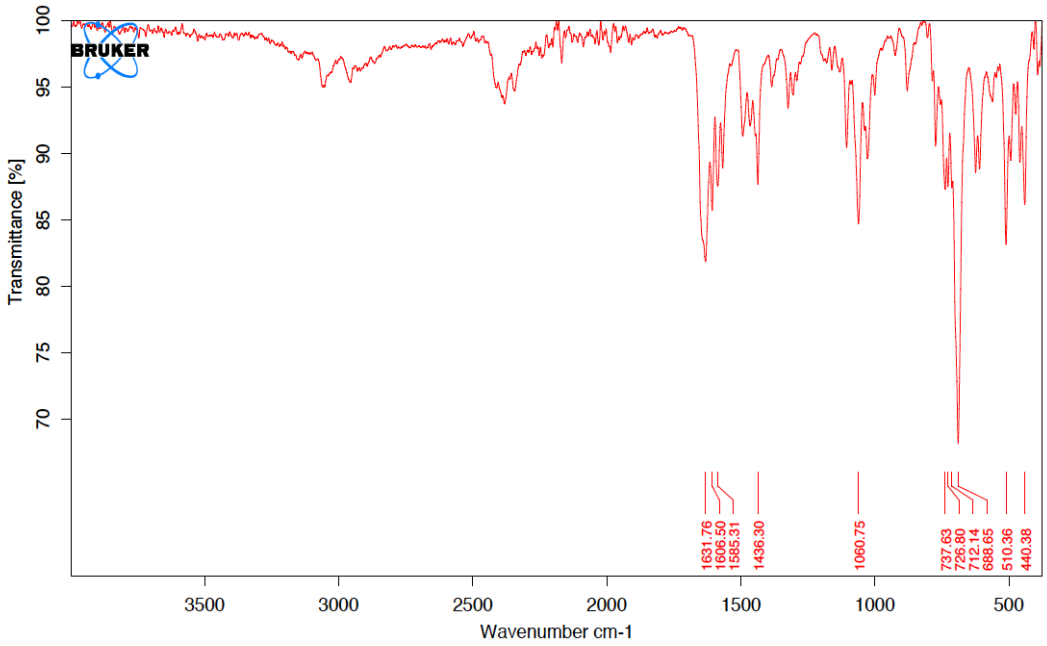

Figure S7. FT-IR spectrum

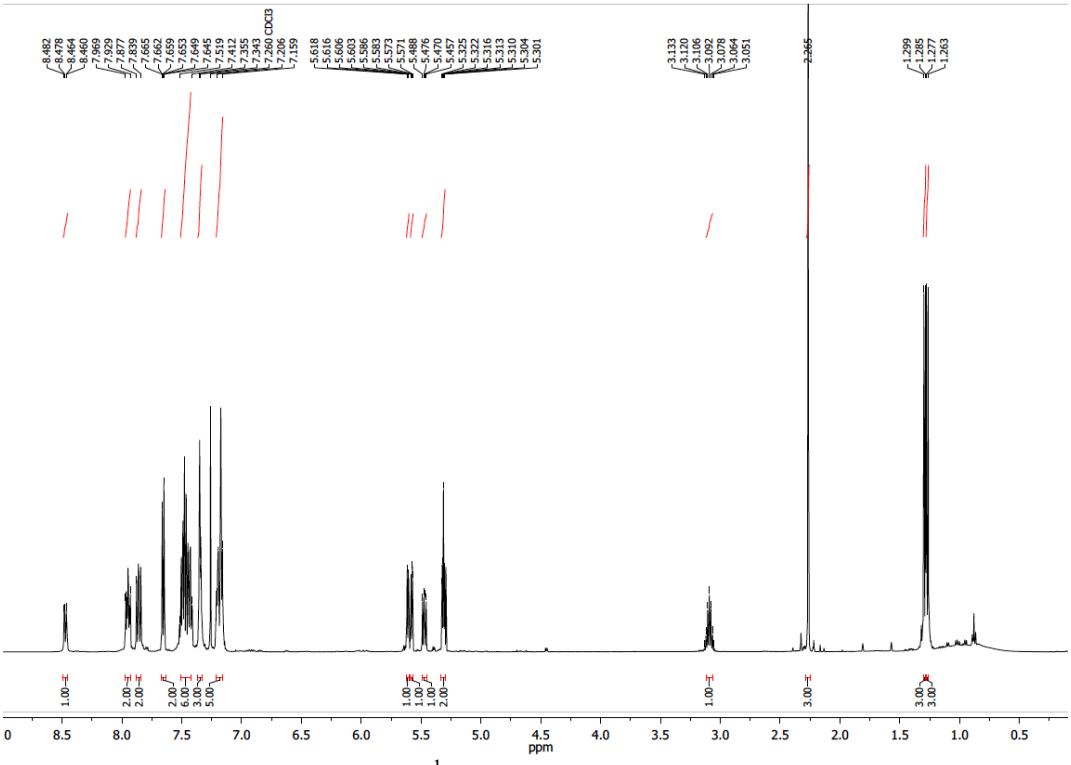

Figure S8. ^{1}H NMR spectrum ($CDCl_3$)

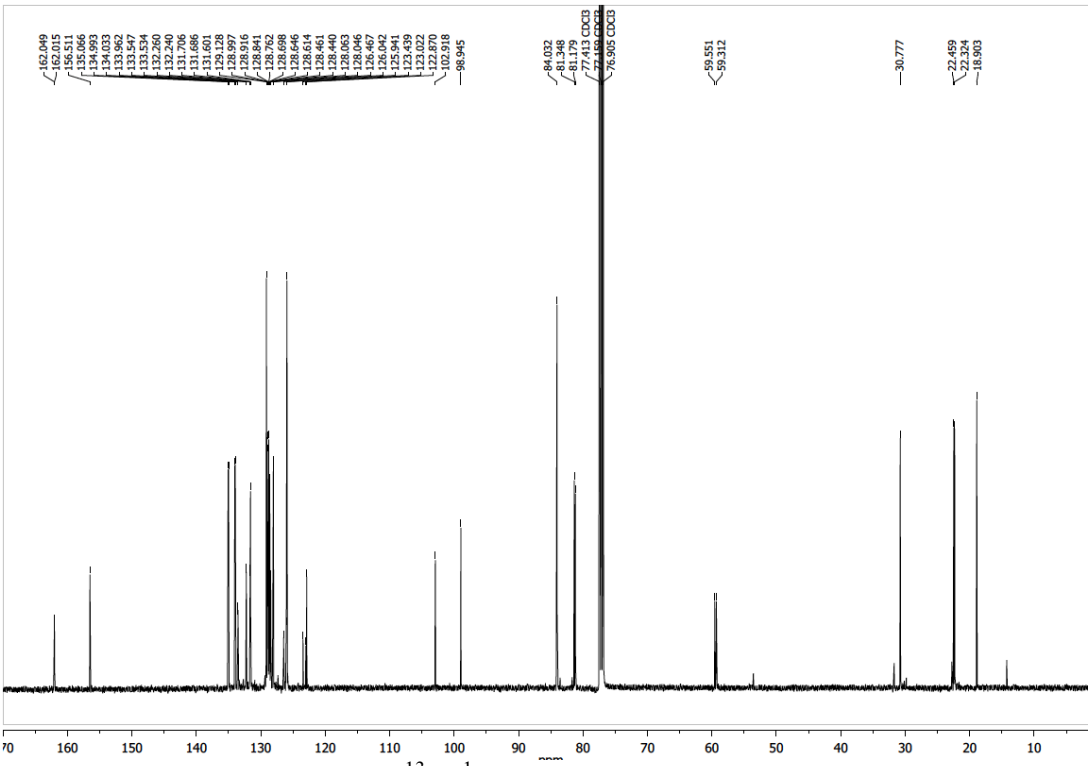

Figure S9. $^{13}C\{^{1}H\}$ NMR spectrum ($CDCl_3$)

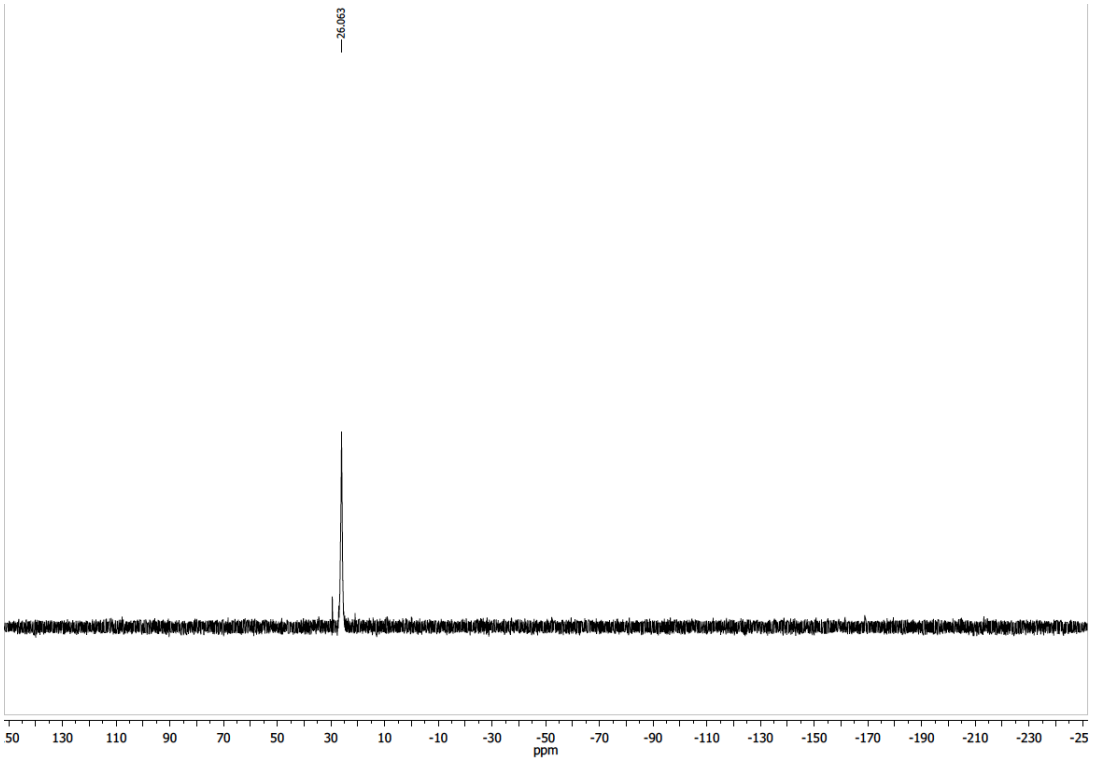

Figure S10. $^{31}P\{^{1}H\}$ NMR spectrum ($CDCl_3$)

Chloro-*P*,*N*-{diphenylphosphanyl-[(5-phenyl-1,3,4-oxadiazol-2-ylamino)phenyl-methyl]}(*p*-cymene)ruthenium(II) hexafluorophosphate (4)

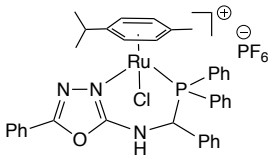

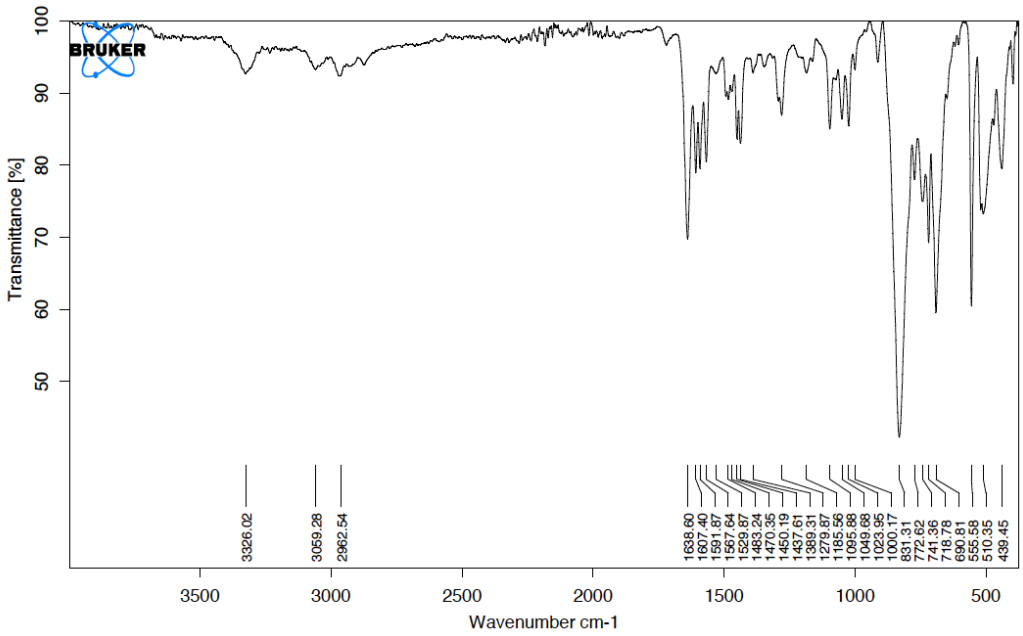

Figure S11. FT-IR spectrum

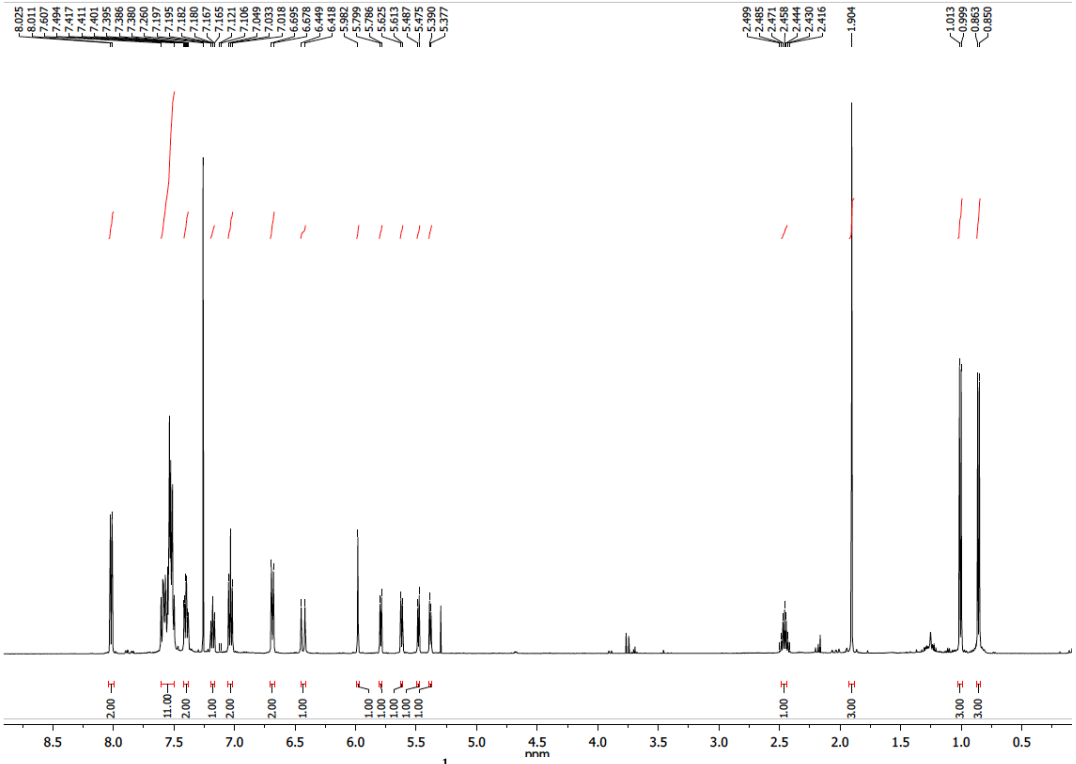

Figure S12. ^{1}H NMR spectrum ($CDCl_3$)

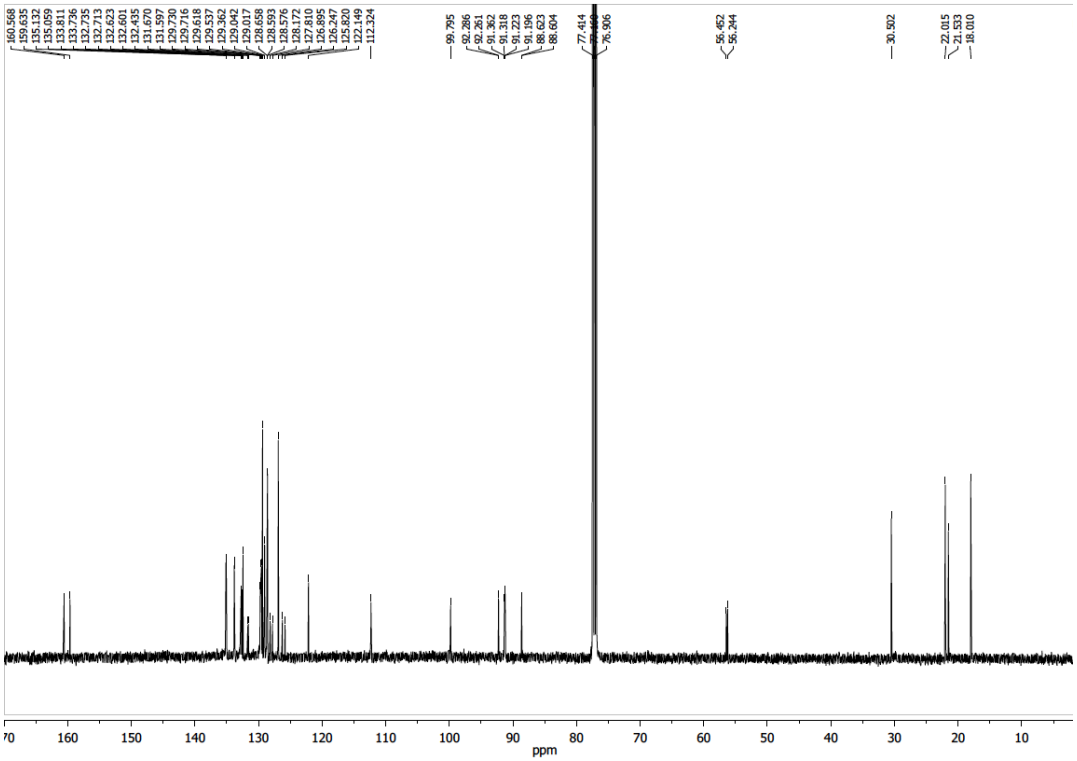

Figure S13. $^{13}C\{^{1}H\}$ NMR spectrum ($CDCl_3$)

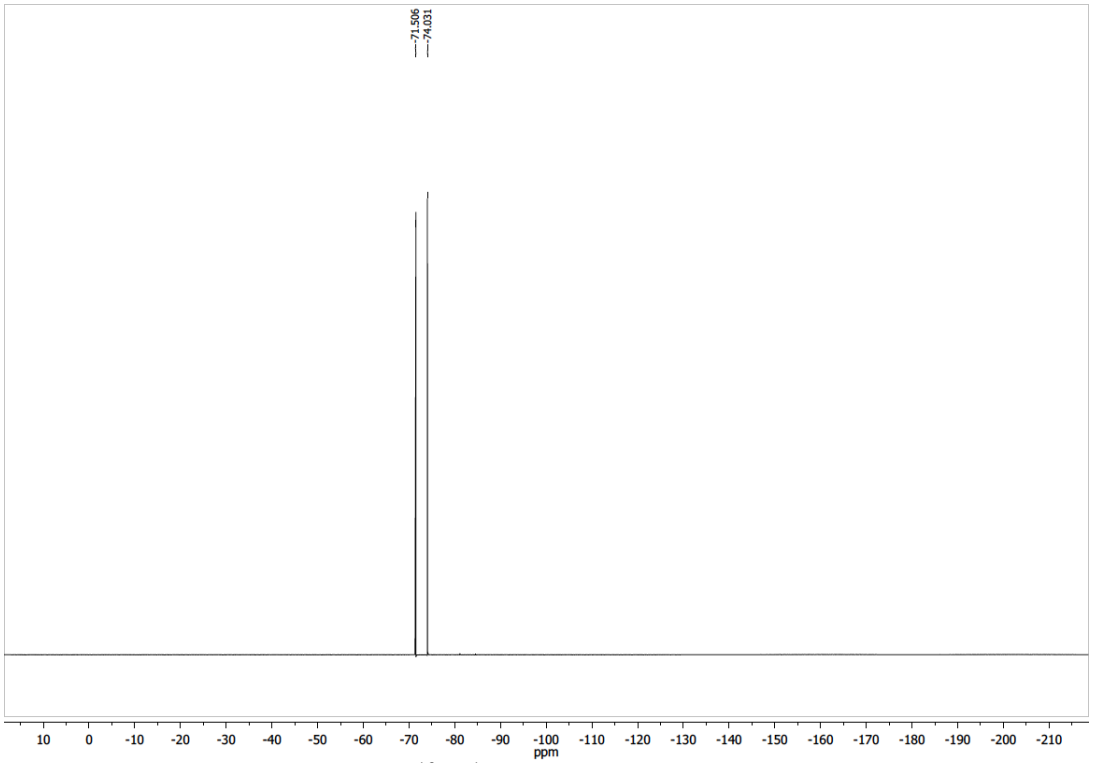

Figure S14. $^{19}F\{^{1}H\}$ NMR spectrum ($CDCl_3$)

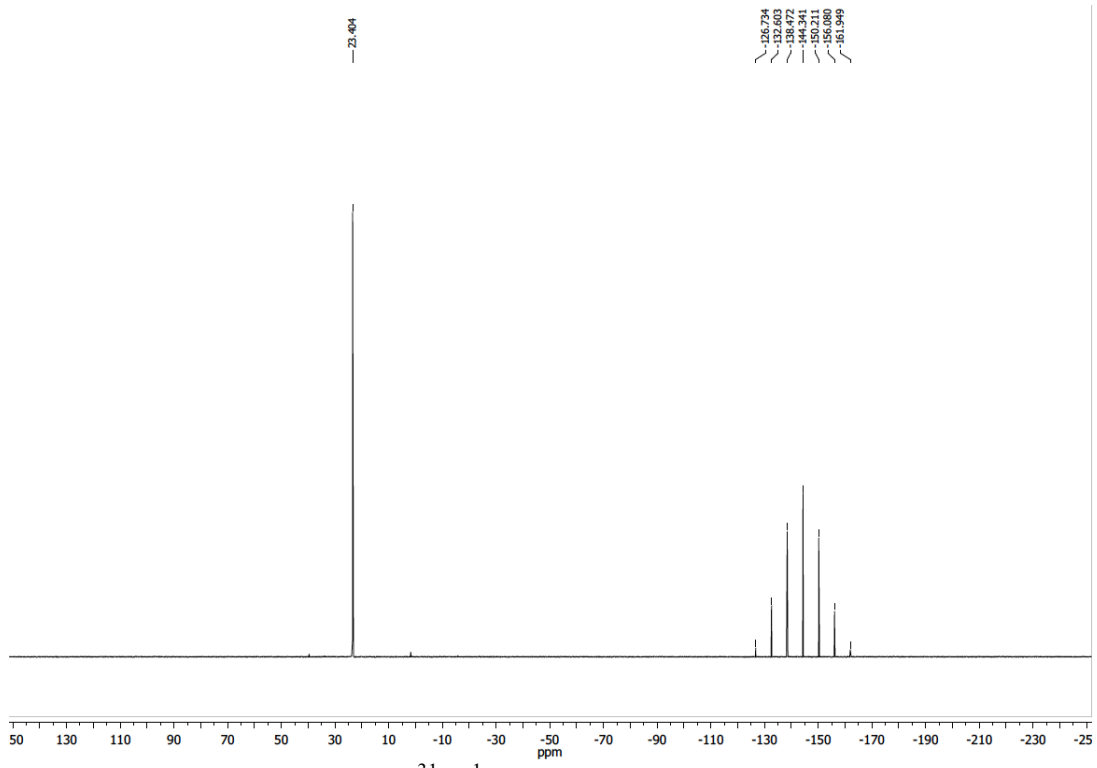

Figure S15. $^{31}P\{^{1}H\}$ NMR spectrum ($CDCl_3$)

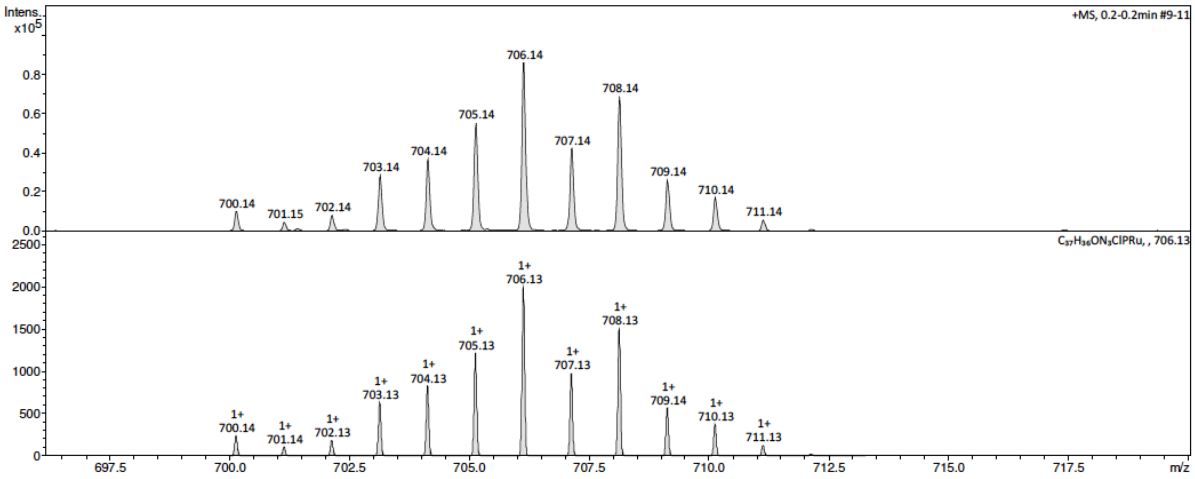

Figure S16. Mass spectrum (ESI-TOF): exp. spectrum (top); calc. spectrum (bottom) for $C_{37}H_{36}ON_3PRuCl$

Packing pattern in the crystal structure

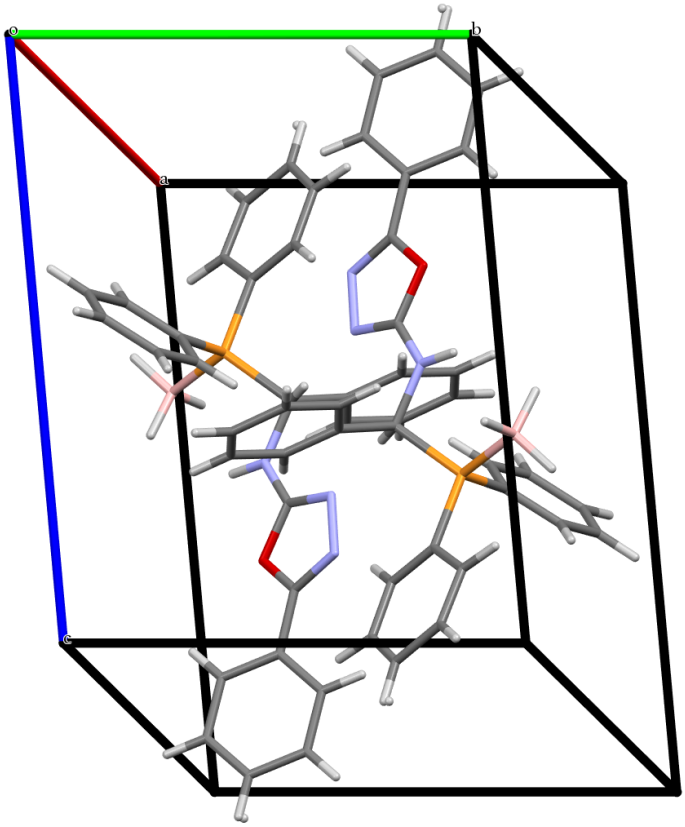

Figure S17. Packing pattern in the crystal structure of compound **2**

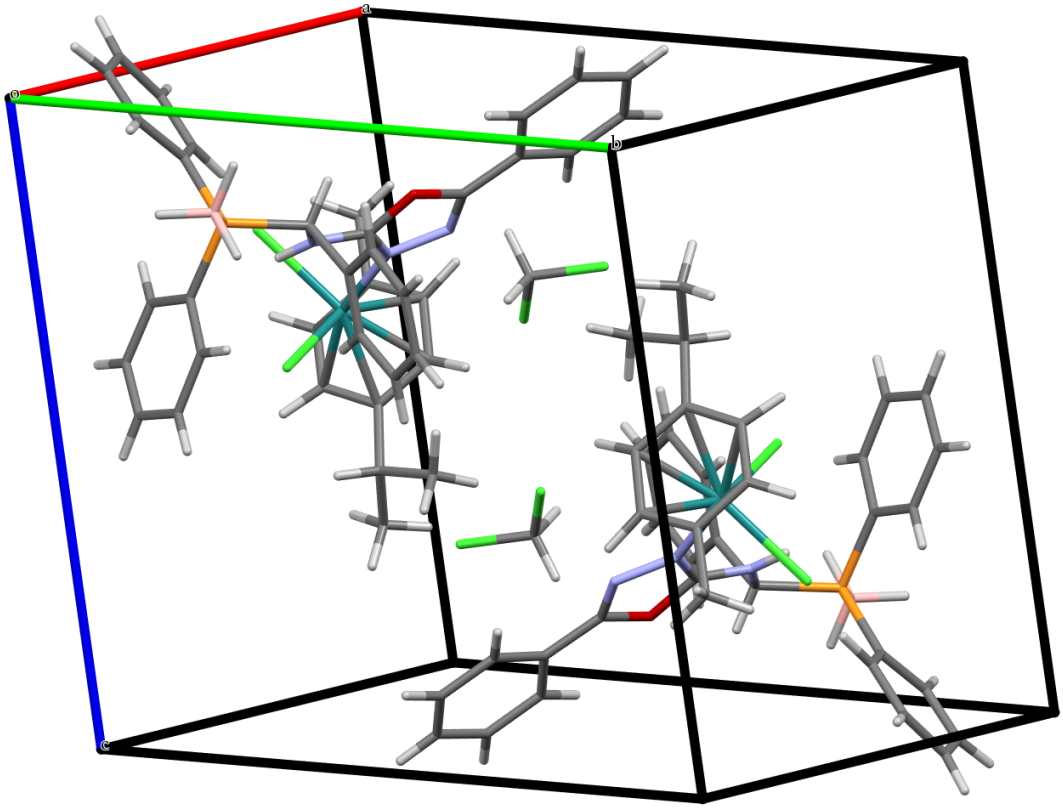

Figure S18. Packing pattern in the crystal structure of complex **3**

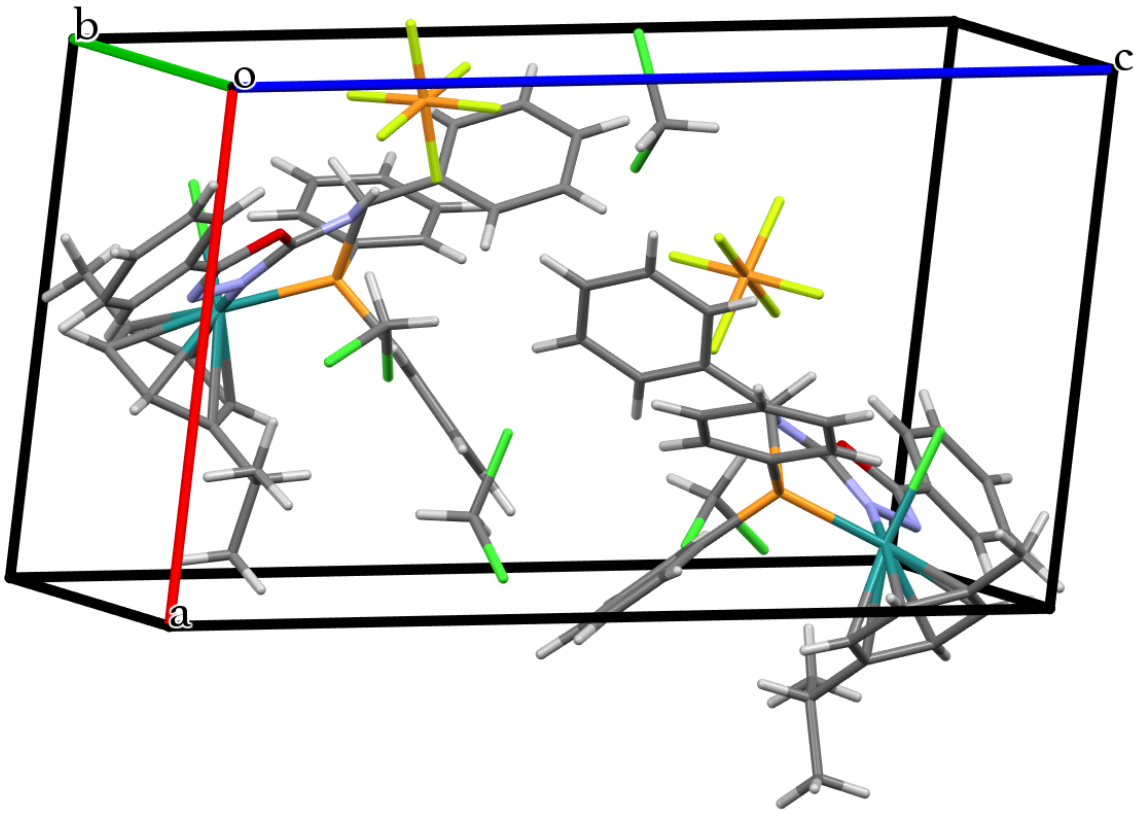

Figure S19. Packing pattern in the crystal structure of complex **4a**

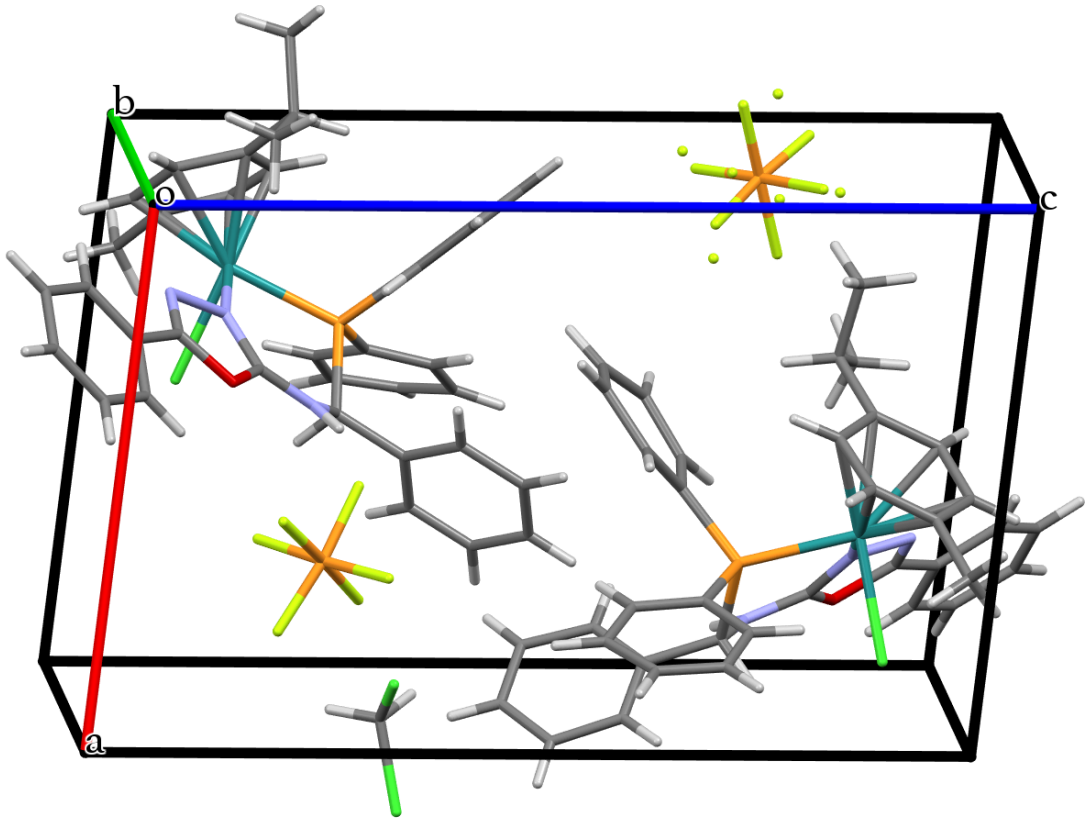

Figure S20. Packing pattern in the crystal structure of complex **4b**

Computational details

All calculations have been performed with the GAUSSIAN 09 (version D01) package [1] at DFT level of theory with the wB97XD functional. All atoms were described by the 6-31+G** basis set except the ruthenium cation which was described by the SDD pseudopotential and associated basis set. Solvent corrections (dichloromethane) were included through a PCM. All geometries were fully optimized and the gibbs free energies extracted from the frequency calculation performed on the geometry minima. Non-Covalent Interaction analyses [2] were performed on the GAUSSIAN wavefunction of the optimized structure using the NCIPlot package.

[1] M. J. Frisch, G. W. Trucks, H. B. Schlegel, G. E. Scuseria, M. A. Robb, J. R. Cheeseman, G. Scalmani, V. Barone, B. Mennucci, G. A. Petersson, H. Nakatsuji, M. Caricato, X. Li, H. P. Hratchian, A. F. Izmaylov, J. Bloino, G. Zheng, J. L. Sonnenberg, M. Hada, M. Ehara, K. Toyota, R. Fukuda, J. Hasegawa, M. Ishida, T. Nakajima, Y. Honda, O. Kitao, H. Nakai, T. Vreven, J. A. Montgomery Jr., J. E. Peralta, F. Ogliaro, M. Bearpark, J. J. Heyd, E. Brothers, K. N. Kudin, V. N. Staroverov, R. Kobayashi, J. Normand, K. Raghavachari, A. Rendell, J. C. Burant, S. S. Iyengar, J. Tomasi, M. Cossi, N. Rega, J. M. Millam, M. Klene, J. E. Knox, J. B. Cross, V. Bakken, C. Adamo, J. Jaramillo, R. Gomperts, R. E. Stratmann, O. Yazyev, A. J. Austin, R. Cammi, C. Pomelli, J. W. Ochterski, R. L. Martin, K. Morokuma, V. G. Zakrzewski, G. A. Voth, P. Salvador, J. J. Dannenberg, S. Dapprich, A. D. Daniels, O. Farkas, J. B. Foresman, J. V. Ortiz, J. Cioslowski, D. J. Fox, *Gaussian 09, Revision D.01, Gaussian Inc*., Wallingford CT, **2009**.

[2] J. Contreras-Garcia, E. R. Johnson, S. Keinan, R. Chaudret, J.-P. Piquemal, D. N. Beratan, W. T. Yang, *J. Chem. Theory Comput*., **2011**, *7*, 625-632.

Table S2. Geometrical parameters of the four ruthenium complexes.

	4a	**5a**	**4b**	**5b**
Ru-Cl (Å)	2.438	2.439	2.438	2.433
Ru-P (Å)	2.340	2.358	2.340	2.336
Ru-N (Å)	2.109	2.128	2.109	2.100
H-C-C-C (°)	-15.4	-22.0	16.2	32.0

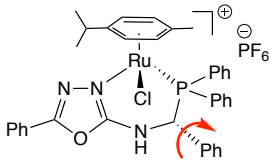

H-C-C-C dihedral angle

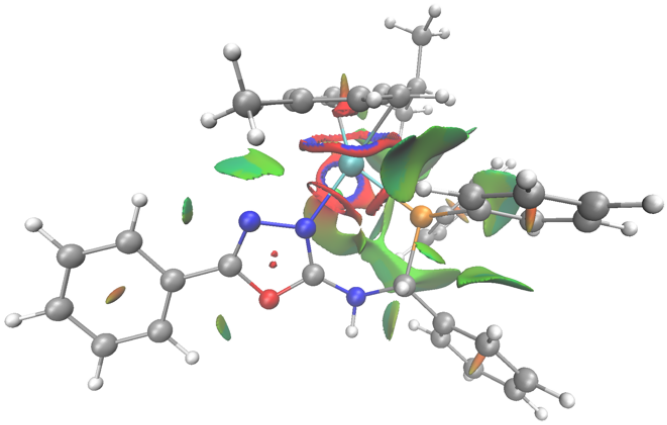

Figure S21. Non-Covalent Interaction analysis of complex **5a**. Green areas represent attractive dispersion forces, red area repulsive steric congestion and blue areas attractive electrostatic interactions.